EARLY LIFE STAGES OF THE SOUTHERN SEA GARFISH, *HYPORHAMPHUS MELANOCHIR* (VALENCIENNES, 1846), AND THEIR ASSOCIATION WITH SEAGRASS BEDS

CRAIG J. NOELL

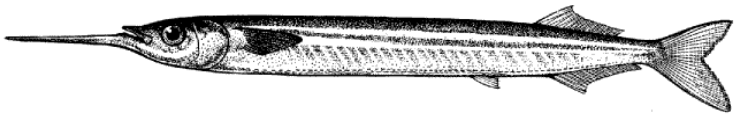

SCHOOL OF EARTH AND ENVIRONMENTAL SCIENCES
THE UNIVERSITY OF ADELAIDE
SOUTH AUSTRALIA

Submitted for the Degree of Doctor of Philosophy
on January 11, 2005

Chapter 1 General Introduction

1.1 BACKGROUND

The southern sea garfish (*Hyporhamphus melanochir*) supports important commercial and recreational fisheries across its distribution in Western Australia (W.A.), South Australia (S.A.), Victoria (Vic.) and Tasmania (Tas.). The most significant commercial fisheries exist in S.A., where, *H. melanochir* is the fourth most valuable finfish within the South Australian Marine Scalefish Fishery after King George whiting (*Sillaginodes punctata*), pink snapper (*Pagrus auratus*) and southern calamary (*Sepioteuthis australis*). The latest figures show that in 2002/2003 the total catch was 332 t and was valued at $1.94 million (unpublished South Australian wild fisheries & aquaculture production figures, South Australian Research & Development Institute[*]). In S.A. there is a high demand for *H. melanochir* in the fresh fish market, restaurant trade and take-away food outlets, with some potential for the value of the fishery to increase with optimal harvesting strategies and product development (Kailola *et al.*, 1993). Furthermore, *H. melanochir* is considered relatively easy to catch and one of the most popular target species in the South Australian recreational fishery. In 1994/95 the recreational catch was estimated at 64 t (McGlennon & Kinloch, 1997). More recently, the estimated recreational harvest had climbed to *c.* 133 t per annum, ranking third behind Australian herring *(Arripis georgianus)* and *S. punctata* (Henry & Lyle, 2003).

The main fishing areas of S.A. for *H. melanochir* are Spencer Gulf and Gulf St Vincent and, to a lesser extent, around Kangaroo Island (Jones & Kangas, 1987). More than 50% of the total commercial harvest is taken from Spencer Gulf and *c.* 40% from Gulf St Vincent (McGlennon & Kinloch, 1997). However, given the difference in the length of coastline of the two gulfs (Spencer Gulf *c.* 1080 km, Gulf St Vincent *c.* 370 km), commercial fishing in S.A. is relatively concentrated in Gulf St Vincent. In the sheltered waters of these areas, *H. melanochir* are closely associated with seagrass beds possibly for feeding and spawning (Jones *et al.*, 1990). The South Australian commercial catch has been relatively stable mostly between 300-500 t per annum since the mid 1960s with large fluctuations in monthly landings being common (Jones & Kangas, 1987; Jones *et al.*, 2002). The majority of this catch has historically been taken by power-hauling nets operated in less than 5 m water depth over seagrass, with dab netting responsible for around 10% of the total catch. However, there is evidence that dab netting has shown a steady increase in harvest share in recent years (Jones *et al.*, 2002). In S.A., haul nets with 3.0-3.2 cm mesh and up to 600 m length are operated in

[*] South Australian Research & Development Institute (SARDI) – Aquatic Sciences, P.O. Box 120, Henley Beach, S.A. 5022.

waters up to 5 m depth (and often over seagrass beds), except northern Gulf St Vincent, where haul netting in deeper water is permitted (since 1987). The recreational fishery for *H. melanochir* includes dab net, and rod and line fishing from boats and jetties throughout the state; of which 65% of the total number are taken from Gulf St Vincent and 33% from Spencer Gulf (McGlennon & Kinloch, 1997). Current output controls for *H. melanochir* caught in S.A. include a minimum legal length of 23 cm total length (implemented in July, 2001, from the previous minimum length of 21 cm) and recreational bag and boat limits of 60 and 180 fish.

In 1995, a national garfish workshop was held at the South Australian Research & Development Institute (SARDI) – Aquatic Sciences, with participants representing research agencies and industry sectors from W.A., S.A., Vic. and Tasmania. A review of the status of the fishery of *H. melanochir* in each state and the biological and fishery information available at that time was followed by an identification of research priorities which would assist future management of this species across its distribution. In general, the literature available on *H. melanochir* was very limited. Despite its commercial and recreational significance, a lack of information has been available to fisheries researchers and managers on the early life history, habitat ecology and population parameters of *H. melanochir*, with reproductive biology and egg and larval development being particularly poorly understood. Consequently, this doctoral program of research on *H. melanochir* was developed to address some of these issues, and was carried out at both SARDI and the Department of Environmental Biology in the School of Earth and Environmental Sciences, The University of Adelaide. It was specifically designed to integrate closely with a larger Fisheries Research & Development Corporation (FRDC)-funded project (Jones *et al.*, 2002) by complementing the relatively straightforward investigation of the fisheries biology of the exploited stock (e.g. age composition, genetic stock discrimination) with a study of the reproductive biology and early life history of *H. melanochir*, including an examination of its relationship with seagrass beds.

1.2 LITERATURE REVIEW

1.2.1 DISTRIBUTION AND TAXONOMY

Hyporhamphus melanochir (Valenciennes, 1846) is endemic to Australian temperate waters. Its geographic distribution extends from Kalbarri in W.A., along Australia's south coast, through Bass Strait and around Tas., to Eden in N.S.W. (Paxton *et al.* 1989). *Hyporhamphus melanochir* are schooling fish, generally found in shallow inshore waters, coastal bays and estuaries, located near the surface at night and close to the bottom over seagrass during the day (Kailola *et al.*, 1993).

Hyporhamphus melanochir belongs to the family Hemiramphidae, commonly known as

the halfbeaks. The Hemiramphidae of Australia and New Zealand include six known genera and 20 species and subspecies (Collette, 1974). The only other hemiramphid that occurs in S.A. is the river garfish (*H. regularis*, Günther, 1886), which may co-occur with *H. melanochir* in estuaries (Jones *et al.*, 1996).

1.2.2 REPRODUCTION AND EARLY LIFE HISTORY

Eight macroscopic stages have been described for female *H. melanochir* gonad development (Ling, 1958). In South Australian waters, spawning is thought to occur from late September to early March, with two distinct peaks in spawning activity from October to November and from January to February (Ling, 1958). St Hill (1996) suggested, in his thesis, that this protracted spawning period is related to *H. melanochir* possibly being serial spawners, with asynchronous oocyte development occurring simultaneously in reproductively active ovaries. Running ripe females are observed in fish at a minimum size of 25 cm fork length (Thomson, 1957*b*; Ling, 1958), and the fecundity of *H. melanochir* is relatively low at about 9000-10000 eggs per individual (Ling, 1958).

Marine hemiramphids are oviparous (Watson, 1996). Ling (1958) described ripe ova of *H. melanochir* as being large, transparent, 2.5-3.5 mm in diameter and "covered by adhesive filaments equal in length to the egg diameter." Large, spherical eggs with adhesive chorion filaments are characters shared among hemiramphids (Collette *et al.*, 1984; Leis & Carson-Ewart, 2000; Watson, 1996), and there have been several observations of different species of hemiramphid eggs attached to fixed or floating objects. Specifically for *H. melanochir*, Jones (1990) noted that eggs coated the meshes of a gill net while sampling adults in spawning condition. Recently, *H. melanochir* eggs were sampled off the east coast of Tas. and were invariably found singly, with their chorionic filaments heavily entangled in filamentous drift algae, mostly at 2-5 m depth (Jordan *et al.*, 1998). These eggs had an average diameter of 2.9 mm with about 100 filaments, each of which were *c.* 8 mm in length.

Jordan *et al.* (1998) successfully reared *H. melanochir* eggs from artificial fertilisation (by stripping running ripe adults) and field-collected samples. Interestingly, when the negatively buoyant eggs were not provided with artificial substrate for attachment, their rate of development was considerably slower and none survived through to hatch. Egg development was described and drawn through to hatching and was shown to have an incubation period of *c.* 30 days at a water temperature of 14-16°C. The same authors also noted that newly hatched larvae are competent swimmers, have a minimal yolk reserve, and must feed within 24 hours. There are two available drawings of *H. melanochir* larvae: one recently hatched specimen of 8.9 mm total length (Jordan *et al.*, 1998) and the other a wild-collected specimen of at least 10.3 mm total length (length type not specified, Bruce, 1989). The latter drawing indicated that development of the characteristic lower beak protrusion among hemiramphids had

already begun in *H. melanochir* larvae of this size.

1.2.3 AGE AND GROWTH

Growth rings in hard parts of fish have been used to obtain estimates of age for a long time. Annual rings were discovered in vertebrae in 1759 (Hederstrom, 1959, cited in Jones, 1992), scales in 1888 (Carlander, 1987), and otoliths in 1899 (Ricker 1975). However, prior to the discovery by Pannella (1971) of daily increments in the otoliths of adult temperate and tropical fish, there was no reliable method for ageing young fish that have not yet formed their first annulus (Jones, 1992). Since Pannella's (1971) discovery, a burgeoning series of scientific papers have appeared where this method has been applied to many larvae, juveniles and short-lived finfish species for the development of age-specific measures of survival and growth (see review by Secor *et al.*, 1992 and references therein). Despite the abundance of literature in this rapidly-growing field, *H. melanochir* larvae have yet to be aged using the daily otolith increment technique. In this study, the ageing of *H. melanochir* larvae is used to describe growth for the South Australian population, which can then be used to back-calculate the hatching dates of individual larvae from their date of capture (Jordan, 1994).

Information on the age and growth of *H. melanochir* is only available for adults, where the well-known method of counting annuli of otoliths was used to obtain estimates of age. Jones (1990) suggested otoliths should be used to determine the age of *H. melanochir* since: 1) scales have indistinct annuli (Ling, 1958) and are easily shed when the fish is handled; 2) there is a lack of prominent modes in length-frequency distributions for older year classes; and 3) tagging is unsuitable due to the high mortality that would exist for such a fragile species. Although Ling (1958) used otoliths to age *H. melanochir*, age was obtained by reading whole otoliths, which can often be underestimated compared to ages obtained from sectioned otoliths. Age-at-length data derived from otolith sections have been used to construct growth curves for *H. melanochir* populations from S.A. (Jones, 1990) and Tas. (Jordan *et al.*, 1998). The growth of *H. melanochir* for both states was shown to be relatively rapid for the first three years until *c.* 27 cm, and thereafter slows considerably until a maximum age of 8-10 years is reached at 33-37 cm.

1.2.4 DIET

There is a considerable amount of literature available on the diet of *H. melanochir*, however, this knowledge pertains to adult fish only. It is unclear at what stage of its life cycle *H. melanochir* begins to feed on seagrass. Thomson (1957*a*) studied the diets of Western Australian estuarine fish species, and found that seagrass (*Zostera* sp.) was the dominant food source for *H. melanochir*. The remainder of the diet was comprised mostly of algae and diatoms. The small amount of animal material found was considered to be incidentally

ingested during herbivory. However, Robertson & Howard (1978) noted that *H. melanochir* sampled at night from Westernport Bay, Vic., contained significantly more amphipods in their guts than during the day. Given that many species of amphipods are benthic during the day, but move up into the water column at night, this indicated that some nocturnal midwater feeding occurs in *H. melanochir*. A more complex feeding pattern emerged when Robertson & Klumpp (1983) discovered that the diet of *H. melanochir* followed a distinct diel cycle from seagrass (*Z. capricorni* and *Z. tasmanica*[†]) during the day to mainly amphipods and other invertebrates at night. They suggested that animals, in particular crustacean zooplankton, are the preferred food for *H. melanochir*, and that seagrass is probably consumed during the day when crustacean prey in the water column is sparse. Klumpp & Nichols (1983) examined the relative contributions of seagrass and zooplankton to the nutrition of this species, and calculated that crustacean prey contributed almost 60% of the daily assimilated energy. The seagrass, which had a relatively quick gut passage time (4.4 h compared to 8.3 h for crustacean food), was assimilated at an efficiency of 38% (organic matter). The crustacea, which was consumed by *H. melanochir* at only a third the quantity of seagrass (and in half the time spent feeding on seagrass), were assumed to be assimilated at an efficiency of 85-98%. The crustacean food was considered "an essential source of protein, and at least as important as seagrass in satisfying the energy requirements of *H. melanochir* (Klumpp & Nichols, 1983)."

The total diet of *H. melanochir* recorded from gut contents includes seagrass, amphipods, insects, polychaetes, natantian larvae, gastropods, other crustaceans (brachyuran larvae, copepods, ostracods, isopods) and algae (Robertson & Howard, 1978; Robertson & Klumpp, 1983; St Hill, 1996). This omnivorous feeding behaviour of *H. melanochir* has also been documented for other hemiramphids including *H. australis* (Thomson, 1959), *Hemiramphus brasiliensis* (Berkeley & Houde, 1978), *H. knysnaensis* (Coetzee, 1981) and *H. ihi* (Saunders & Montgomery, 1985).

Hyporhamphus melanochir feeds on large quantities of seagrass, yet like all hemiramphids it has a simple straight tubular gut without a stomach or appendages (Suyehiro, 1942), and its relative gut length of only 0.5 (Robertson & Klumpp, 1983) is atypical of an herbivore. Ingested seagrass is thoroughly macerated, presumably by the action of a pharyngeal mill that is present in hemiramphids (Tibbetts, 1991). The resultant seagrass 'juice' is apparently assimilated with 100% efficiency (Klumpp & Nichols, 1983). It has been proposed that some hemiramphids have developed a mucous-mediated absorption mechanism

[†] In their revision of the systematics of seagrasses (Zosteraceae) in Australia and New Zealand, Les *et al.* (2002) recommend that the species *Zostera muelleri* and *Heterozostera tasmanica* be termed *Z. capricorni* and *Z. tasmanica*, respectively. In accordance with the change in nomenclature, the latter species' names are adopted throughout this thesis.

for more efficient extraction of nutrients from mechanically digested plant material (Tibbets, 1997).

1.3 SIGNIFICANCE OF SEAGRASS TO *H. MELANOCHIR*

Seagrasses are found in sheltered coastal waters around the world and approximately half the total number of seagrass species occur in the coastal waters of Australia (Kirkman & Walker, 1989). It is widely regarded that seagrass provides an important habitat within the marine ecosystem for its associated fauna. The importance of seagrass to its fauna inhabitants include the provision of nursery, feeding and spawning areas and refuge from predators for many species of fish (Bell & Pollard, 1989). Furthermore, seagrass beds support processes and functions within the marine environment by trapping sediment, stabilising the seabed, reducing coastal erosion and providing a basis for the marine food web through photosynthesis. While fish densities in seagrass beds are not always higher than adjacent bare substrata, most studies have shown that seagrass has a positive affect towards increasing the richness and abundance of associated fish assemblages (Bell & Pollard, 1989 and references therein; Connolly, 1994; Edgar & Shaw, 1995*a*). Therefore, the large-scale degradation or dieback of seagrass in many areas is cause for concern in regards to sustainability of fish, including economically important species, which have significant links with seagrass for part of their life cycles (Shepherd *et al.*, 1989; Edgar *et al.*, 1994; Jenkins *et al.*, 1997; Seddon, 2000).

Specifically for *H. melanochir*, there is the perception that this species has a strong linkage with seagrass for much of its life history since commercial fishers target *H. melanochir* in areas that are often dominated by the zosteracean seagrasses "garweed" *(Z. capricorni*) and "eelgrass" (*Z. tasmanica*), significant quantities of seagrass are often found in the guts of adult *H. melanochir* (Robertson & Klumpp, 1983), and the eggs of *H. melanochir* are covered with long chorionic filaments presumably used for attachment to seagrass or some other vegetation (Ling, 1958; Jordan *et al.*, 1998). Therefore, there are many possible ways in which *H. melanochir* might be reliant upon seagrass beds for some aspect of their life cycle or physiology. If this is the case, then the continual loss of seagrass in inshore areas of S.A. (and elsewhere – notably Vic., Jenkins *et al.*, 1997), particularly along the Adelaide metropolitan coast where a significant part of the *H. melanochir* fishery is located, would have detrimental effects on *H. melanochir* populations and threaten the ability of this resource to sustain a viable fishery in the long term (Seddon, 2001). This research program examines the possible association of early life stages of *H. melanochir* with seagrass from a biological perspective in comparison to an empirical mathematical relationship developed by Scott *et al.* (2000), who demonstrated using a 'seagrass residency index' (SRI) that, out of all the

important commercial and recreational marine scalefish species in S.A., *H. melanochir* was the species most likely to be adversely affected by changes in the health and abundance of seagrass beds.

1.4 OVERALL AIMS AND STRUCTURE OF THESIS

The scope of the original proposal was quite broad, thus allowing flexibility into the type of research conducted and the lines of enquiry pursued. The overall aims of this study are to describe the early life stages of *H. melanochir* and to explore the possible relationship(s) between the various life stages and seagrass habitat with the emphasis on seagrass as a requirement for spawning or as an assimilated direct food source. The importance of seagrass for spawning is inferred by linking the abundance and distribution of larvae in Gulf St Vincent with the extent of seagrass cover, prevailing winds in the gulf, and the age and growth of larvae (Chapter 5). Its importance to the diet of various life stages is examined by an empirical comparison of the stable isotope signatures of potential food sources and tissue of *H. melanochir* itself (Chapter 6). Before the relationship with seagrass is addressed, it was deemed necessary to update some of Ling's (1958) work on the reproductive biology of *H. melanochir* with the addition of histological information for a more accurate assessment of ovarian development and to examine the significance of the morphology of the oocyte (Chapter 2). Furthermore, since the collection of *H. melanochir* larvae is a critical step in establishing links with habitat, molecular tools are used to verify that aprioristically identified larvae are in fact *H. melanochir* (Chapter 3). The morphology of *H. melanochir* larvae is then described and drawn so that larvae can be accurately identified from field-collected specimens (Chapter 4). Both Chapters 3 and 4 also include the identification and description of *H. regularis* larvae so that both species can be genetically and morphologically distinguished from one another.

Knowledge of the reproductive biology, early life history, and habitat ecology of *H. melanochir* is critical for our understanding of the spawning behaviour and life strategies adopted by this species to propagate itself for future generations. Accordingly, early life strategies can be compared with other species, and benefits and trade-offs in adopting particular strategies can be explained. It is expected that this type of information would benefit researchers and managers in the development of population models and formulation of accurate stock assessments for this species. For example, more information on spawning areas, egg and larval distributions, and habitat requirements of these early life stages would provide for a better understanding of the factors that may influence year-class variability and ultimately the prediction of recruitment strength into the exploitable population. It is anticipated that results from this thesis, in association with fisheries biological information on

adult populations of *H. melanochir* (Jones *et al.*, 2002), will facilitate well-informed management decisions for the fishery from a scientific perspective.

1.5 OBJECTIVES

In order to address the overall aims of this thesis, and given the paucity of information described above, the following specific objectives were developed:

1. (a) Describe the different stages of oocyte development and the dynamics of their development; (b) establish whether the filaments associated with the oocyte surface are adhesive; (c) determine the sex ratio; (d) confirm the duration of the spawning season; (e) determine size at sexual maturity; and (f) estimate batch fecundity. *{Chapter 2}*
2. (a) Develop a multiplex PCR assay that discriminates between life stages of *H. melanochir* and *H. regularis* in southern Australia based on the presence/absence of diagnostic bands; and (b) verify the assay on an extensive sample of adults of each species. *{Chapter 3}*
3. (a) Describe the larval development of *H. melanochir* and *H. regularis*; and (b) document distinguishing characters between larvae of each species. *{Chapter 4}*
4. (a) Determine broad spawning area patterns in Gulf St Vincent from the distribution and abundance of *H. melanochir* eggs and larvae; (b) confirm that *H. melanochir* larvae are concentrated in the neuston; (c) back-calculate hatching dates through the determination of the age and growth of larvae; and (d) assess the reliance upon seagrass for spawning by *H. melanochir* with the aid of comprehensive benthic habitat maps of the gulf. *{Chapter 5}*
5. Quantify the importance of zosteracean seagrass towards the assimilated diet of different life stages of *H. melanochir* by dual stable isotope analysis ($\delta^{13}C$, $\delta^{15}N$) of larval, juvenile and adult *H. melanochir* and several potential food sources. *{Chapter 6 }*

Chapter 2 Reproductive biology[‡]

2.1 INTRODUCTION

A diversity of reproductive strategies has evolved among teleost fishes to maximise reproductive success within the environment to which each species has become adapted (Wallace & Selman, 1981). This diversity is reflected in differences in the cellular processes of oocyte development, the size of the oocytes, the dynamic organisation of oocytes within the ovary, and reproductive pattern, i.e. hermaphroditic or gonochoristic (deVlaming, 1983). Knowledge of the reproductive strategy of a commercially exploited species contributes to understanding its population dynamics, which is fundamental in the development of management and conservation measures that ensure sustainability of the fishery (Fowler *et al.*, 1999).

This study focuses on the reproductive biology of *H. melanochir*. Common to most marine hemiramphids, the eggs of *H. melanochir* are large, demersal, and become attached to benthic seagrass or algae by their chorionic filaments (Collette *et al.*, 1984; Jordan *et al.*, 1998). Newly-hatched larvae appear to be competent swimmers and are found in the neuston throughout estuarine and gulf waters of S.A. (Jordan *et al.*, 1998; Chapter 5).

Reproductive studies of *H. melanochir* thus far have provided information on time of spawning, size at maturity, sex ratio, and fecundity for populations from W.A. (Thomson, 1957*b*), S.A. (Ling, 1958) and Tas. (Jordan *et al.*, 1998). However, until recently (McBride & Thurman, 2003), no reproductive study of *H. melanochir* or any other hemiramphids (Talwar, 1962*b*; Talwar, 1967; Berkeley & Houde, 1978; Aoki, 1988; Durai *et al.*, 1988) has considered the histological examination of ovaries. McBride & Thurman (2003) updated the work of Berkeley & Houde (1978) on *Hemiramphus brasiliensis* and *He. balao* by providing new histological information. Similarly, the present study updates the work of Ling (1958) on the reproductive biology of female *H. melanochir* from S.A. with the addition of histological information augmented by macroscopic data. Although histological methods are time-consuming and expensive, they give the most accurate assessment of ovarian development in fishes (West, 1990).

[‡] The results presented in this chapter focus solely on *H. melanochir* populations from Gulf St Vincent and were derived from a collaborative study on populations from across southern Australia with Dr Qifeng Ye, David McGlennon and David Short from SARDI Aquatic Sciences, and thus constitute part of the following report chapter:
Ye, Q., Noell, C. & McGlennon, D. (2002). Reproductive biology of sea garfish. In Fisheries biology and habitat ecology of southern sea garfish (*Hyporhamphus melanochir*) in southern Australian waters (Jones, G. K., Ye, Q., Ayvazian, S. & Coutin, P., eds), pp. 209-253. FRDC Project 97/133. Canberra, Australia: Fisheries Research and Development Corporation.

In addition, the chorionic filaments of oocytes were examined using histological and electron microscopic techniques to determine whether they are adhesive or not. A number of studies, many on the extracellular material of bacteria, have referred to an adhesive substance as a 'glycocalyx,' which is mucopolysaccharide in nature (Fletcher & Floodgate, 1973; Herald & Zottola, 1988; Barber *et al.*, 1993; Fassel *et al.*, 1998). Consequently, oocytes were stained for the presence of this glycocalyx to determine whether eggs can attach to vegetative substrate via adhesion as well as entanglement.

In describing the reproductive biology of *H. melanochir*, the population from northern Gulf St Vincent were investigated as this is an important region of the South Australian fishery. Specific objectives were to: (a) describe the different stages of oocyte development and the dynamics of their development; (b) determine whether the filaments on the oocyte surface are adhesive; (c) to determine the sex ratio; (d) confirm the duration of the spawning season; (e) determine size at sexual maturity; and (f) estimate batch fecundity.

2.2 MATERIALS AND METHODS

2.2.1 COLLECTION OF FISH

A total of 2000 fish were analysed from the inshore waters of Gulf St Vincent, S.A., north of 34°11'S latitude, from October 1998-May 2000 and during December 2001. Subsamples of up to 50 fish were purchased from commercial processors approximately weekly during the expected spawning season (October-March) and monthly during the non-spawning season (April-September). These fish were kept on ice since capture and received for laboratory processing within 24 h. All fish were from commercial catches caught with power-haul nets operated in depths <5 m and subjected to old and new legal minimum lengths of 210 and 230 mm L_T, respectively. This change in legal minimum length for *H. melanochir* was implemented in S.A. in July 2001.

2.2.2 LABORATORY PROCEDURES

2.2.2.1 Processing of fish

Fish were measured for standard length (L_S) and maximum L_T to the nearest 1 mm, and weighed (W_T) to 0.1 g. The lobes of the caudal fin were compressed dorso-ventrally to obtain maximum L_T (hereafter simply referred to as L_T) (Anderson & Gutreuter, 1983). Gonads were removed, sexed, and weighed to the nearest 0.01 g (W_G). The gonadosomatic index (I_G) was calculated as $(W_G/W_F) \times 100\%$, where W_F is gonad-free fish weight (i.e. $W_T - W_G$). Males were excluded from further analysis since the development of testes is generally less

pronounced than ovaries (West, 1990) and it was assumed that the spawning cycle is synchronous between sexes.

Each ovary was classified macroscopically to one of eight stages of development based on visibility, size, and colour of oocytes using the criteria of Ling (1958) (TABLE 2.1). For those ovaries classified as mature (i.e. stage III and above), 20 fresh oocytes of the largest size class were teased out and their diameters measured on a random orientation basis to obtain an average maximum diameter. Oocytes were measured using SigmaScan Pro® 5.0 image measurement software to an accuracy of <20 μm (SPSS Inc., 1999*a*). Hydrated oocytes stood out as a discrete and easily identified group and were therefore used to estimate batch fecundity (F_B) by the gravimetric method (Hunter *et al.*, 1985). When oocyte diameters were >2200 μm (an arbitrarily chosen diameter at which oocytes are hydrated), a *c*. 25-mm segment was removed from the middle of an ovarian lobe, weighed to 0.0001 g (W_S), and hydrated oocytes were counted (F_S). Batch fecundity was calculated for the combined weight of both ovaries using the equation $F_B = (F_S/W_S) \times W_G$.

TABLE 2.1 Descriptions of the eight macroscopic stages of development of the ovaries of *Hyporhamphus melanochir* (modified with permission from Ling, 1958).

Stage	Classification	Macroscopic description
I	Immature virgin	Gonads small and threadlike, extending about ⅓ the length of the body cavity, sometimes only just visible. Impossible to distinguish sex.
II	Developing immature virgin	Ovaries small and thin, about 1.5 mm in diameter, occupying same length of the body cavity as Stage I. No oocytes visible.
III	Mature virgin or resting spent	Ovaries about 3 mm in diameter, extending about ½ the length of the body cavity. A blood vessel runs along the dorsolateral surface with smaller vessels ramifying over the posterior region. Small white oocytes just visible in transparent ovaries.
IV	Mature	Ovaries about same relative length as for Stage III but twice the diameter. Blood vessels larger. Oocytes clearly visible, with a diameter of about 1 mm.
V	Mature	Ovaries about 8 mm in diameter, extending about ¾ the length of the body cavity. Blood vessels ramifying over the ovaries are reduced, but the main dorsolateral ones still large. The oocytes appear to be clearing and are 1.5 mm in diameter.
VI	Ripe	Ovaries have become much swollen to about 18 mm in diameter, extending the entire length of the body cavity. Only the large lateral blood vessels obvious. Ripe oocytes 2.5-3 mm in diameter appear as a clear, yellow-green, jelly-like mass and are quite firmly packed, the ovary being fairly turgid. There is no sign of the genital pore being open. Smaller oocytes constitute a second group.
VII	Running ripe	Ovaries may be somewhat flaccid if some oocytes have been shed. Lateral blood vessels are still large and clearly defined. Oocytes shed through genital pore when slight pressure is applied to the abdomen.
VIII	Spent	Ovaries shrunken and flaccid, may be bloodshot. Tunica tough, unlike easily ruptured ovarian wall of preceding ripe stages. Blood begins to appear at the posterior end where ramifying vessels were obvious in earlier stages. Some residual oocytes may be apparent, but many 'medium-sized' oocytes of the next smallest group still visible.

Oocyte size-frequency distributions were derived from at least five ovaries representing each of stages II-VII (sex is macroscopically indistinguishable for stage I). An ovarian lobe was split longitudinally and placed in a modified Gilson's solution for at least 24 h and periodically shaken with vigour (Snyder, 1983). This fixative hardens oocytes and chemically separates them from ovarian connective tissue. The oocytes were washed from the ovarian matrix and collected in a 50-μm sieve, similar to that devised by Lowerre-Barbieri & Barbieri (1993), and stored in 70% ethanol for one week. A subsample was then taken, from which diameters of preserved oocytes were measured and volumes calculated [vol. of sphere = (4/3) $\pi \times \text{radius}^3$]. Although Gilson's solution has been found to destroy hydrated oocytes (Lowerre-Barbieri & Barbieri, 1993 and references therein), no such problem was experienced in this study. However, to obtain estimates of shrinkage caused by Gilson's, a number of oocytes from ovarian stages II-VII were measured before and after preservation (<2200 μm, n = 80; >2200 μm, n = 40). For histological preparation, another mid-ovarian segment was removed and fixed in a solution of 10% formalin, 5% acetic acid and 1.3% calcium chloride.

2.2.2.2 Histological preparation

Ovarian segments were dehydrated in a graded ethanol series and embedded in paraffin wax. Prior to sectioning, tissue blocks were immersed in ice water for 10 min to soften the trimmed face and prevent sections shattering. Tissue was sectioned transversely at 3-μm thickness, and stained either with haematoxylin and eosin or by the combined alcian blue-periodic acid-Schiff (AB-PAS) reaction. The AB-PAS stain was used to investigate whether the filaments associated with the oocyte surface are coated with an adhesive substance through the demonstration of mucopolysaccharides (Mowry, 1956). Terminology for describing oocyte development follows that given by West (1990) (TABLE 2.2). Slides were examined at 40-400× magnifications. Measurements using an eyepiece micrometer were only taken from histological preparations if oocytes were sectioned through the nucleus. However, measurements of oocyte diameters are for comparison only, and should only be interpreted after taking into consideration the shrinkage and distortion caused by dehydration and the bias introduced when oocytes are not sectioned at their largest diameter (West, 1990).

2.2.2.3 Transmission electron microscopy

Transmission electron microscopy (TEM) was also used to examine the oocyte filaments for adhesiveness at ultra high magnifications. For the control procedure, oocytes were fixed overnight at 4°C in 4% paraformaldehyde, 5% glutaraldehyde and phosphate-buffered saline with 4% sucrose (PBS) at pH 7.2 (Guandalini *et al.*, 1994). The material was then washed in PBS for 2 × 20 min, post-fixed in 1% osmium tetroxide for 1 h, dehydrated in a graded

TABLE 2.2 Brief descriptions of stages of oocyte development in teleosts (from West, 1990).

Oocyte stage	Histological description
Perinucleolar	Nucleus increases in size and multiple nucleoli appear at its periphery. Formation of the zona radiata of the chorion begins in this stage or the yolk vesicle stage.
Yolk vesicle	Appearance of yolk vesicles in the cytoplasm. Yolk vesicles (often referred to as cortical alveoli) increase in size and number to form several rows.
Yolk globule	Appearance of yolk proteins in fluid-filled spheres (referred to as yolk globules, granules or spheres), marks the beginning of vitellogenesis, i.e. the formation of yolk.
Migratory nucleus	Peripheral migration of the nucleus and its dissolution, often accompanied by coalescence of yolk globules.
Hydrated	Rapid increase in size of oocyte due to hydration. Cytoplasm appears homogeneous.

ethanol series and embedded in Epon-Araldite®. For specific demonstration of mucopolysaccharides, and therefore adhesiveness, oocytes taken from the same ovary as the control oocytes were processed following the same protocol with the addition of 0.15% ruthenium red (RR) to both the primary and post fixatives (Barber *et al.*, 1993). Propylene oxide was incorporated at the final dehydration step to facilitate infiltration of the embedding medium. Ultra-thin sections were stained with uranyl acetate and lead citrate (Reynolds, 1963) and examined with a Philips CM100 TEM at 80 kV accelerating voltage.

2.2.3 STATISTICAL ANALYSES

A single-factor analysis of variance (ANOVA) was used to test for significant shrinkage of mean oocyte diameter before and after Gilson's treatment. A chi-square (χ^2) goodness of fit (Zar, 1999) was used to test whether sex ratio significantly deviated from 1:1. A binary logistic function, where mature fish were assigned a value of 1 and immature fish 0, was fitted to estimate the probability P_M that a female of a given L_S collected during the spawning season has mature ovaries using the LOGIT module in SYSTAT® 9 (Steinberg & Colla, 1999). The logistic function is $P_M = 1/[1 + e^{-(a+bL_S)}]$, where a and b are regression coefficients. The length at sexual maturity (L_{50}), defined as the L_S at which $P_M = 0.5$, was derived from the equation $L_{50} = -a/b$. All regressions of fecundity against fish size were tested for significance by ANOVA. Conversions between L_S and L_T were calculated according to the relationships: $L_S = 0.872\ L_T - 2.372$ and $L_T = 1.143\ L_S + 3.548$ ($n = 1063$, $r^2 = 0.997$, $P<0.001$).

2.3 RESULTS

2.3.1 STAGES OF OOCYTE DEVELOPMENT

2.3.1.1 Perinucleolar stage [FIG. 2.1(b), (c)]

Diameter 25-210 μm; *n* = 90 oocytes, 6 ovaries. Early-stage oocytes are irregularly shaped (spherical to elongated and often angular), depending on the pressures of surrounding oocytes of various stages. The cytoplasm has a grainy appearance and is strongly basophilic, staining purple, while in contrast, the nucleus is weakly basophilic. The diameter of the nucleus is more than half that of the cytoplasm and contains multiple densely stained nucleoli, usually located around the periphery. Late-stage oocytes tend to be more regularly shaped. Hereafter, the cytoplasm loses its affinity for haematoxylin. The nucleus starts to become acidophilic, staining pale pink, and its diameter is about one-third that of the oocyte. The nucleus-to-cytoplasm ratio continues to decrease throughout the following stages. Formation of the granulosa and thecal cells of the follicular layer begins during the latter part of this stage. In some oocytes, precursor material for the zona radiata can be seen at 400× magnification as a thin pink line delineating the follicular layer from the cytoplasm.

2.3.1.2 Yolk vesicle formation [FIG. 2.1(d), (e)]

Diameter 162-525 μm; *n* = 48 oocytes, 5 ovaries. This stage is characterised by the presence of clear yolk vesicles in the cytoplasm, which appear as vacuoles. Yolk vesicles are randomly distributed; they increase in size and number until they occupy the whole cytoplasm. The outline of the nucleus becomes irregular. The zona radiata first appears in early-stage oocytes and gradually increases in thickness to *c*. 10 μm. It is acidophilic, staining pink. Filaments surrounding the oocyte also appear and they too are acidophilic, originating from the zona radiata. In section, the filaments appear to be in furrows outside the zona radiata, which initially has an irregular surface but later becomes smooth. They are situated beneath the thecal cells and interspersed among the granulosa cells. Because the filaments are tapered towards their ends and sections are cut at various angles to their alignment, both size and shape of filaments appear variable in section.

2.3.1.3 Yolk globule stage [FIG. 2.1(f)]

Diameter 323-596 μm; *n* = 24 oocytes, 5 ovaries. This stage represents the beginning of vitellogenesis. Small acidophilic yolk globules first appear in the inner region of the cytoplasm. These increases in size and number, gradually spreading outwards, and at the same time displacing the yolk vesicles toward the periphery of oocytes. The zona radiata progressively increases in thickness to *c*. 20 μm.

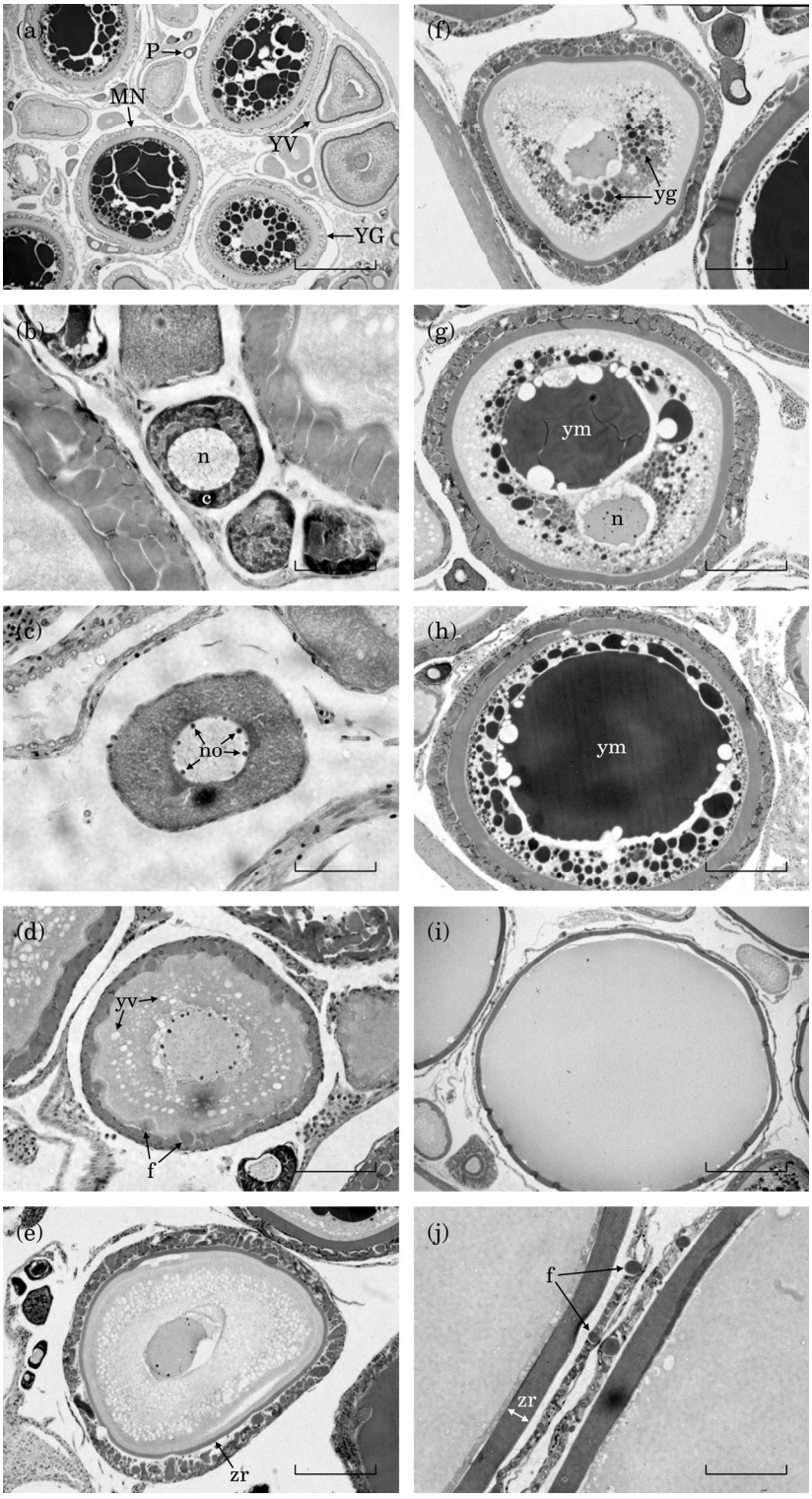

FIG. 2.1 Histological features of ovarian and oocyte development for *Hyporhamphus melanochir* stained with haematoxylin and eosin. (a) Partial cross section of a stage III ovary showing the presence of all oocyte stages except hydrated; (b) Early perinucleolar; (c) late perinucleolar; (d) early yolk vesicle; (e) yolk vesicle; (f) yolk globule; (g) migratory nucleus; (h) late migratory nucleus; (i) hydrated; (j) enlargement of detail of hydrated. Abbreviations: *P* perinucleolar; *YV* yolk vesicle; *YG* yolk globule; *MN* migratory nucleus; *c* cytoplasm; *f* filaments; *n* nucleus; *no* nucleoli; *yg* yolk globules; *ym* yolk mass; *yv* yolk vesicles; *zr* zona radiata. Scale bars: (a), (i) 500 µm; (b), (c) 50 µm ; (d), (j) 100 µm; (e), (f), (g), (h) 200 µm.

2.3.1.4 Migratory nucleus stage [FIG. 2.1(g), (h)]

Diameter 580-1310 μm; *n* = 46 oocytes, 5 ovaries. Yolk globules coalesce to form a yolk mass, and this occurs simultaneously with the migration of the nucleus to the periphery of the oocyte and its subsequent dissolution. The zona radiata is very distinct, measuring 30-60 μm in thickness and showing a fine lamellar appearance.

2.3.1.5 Hydrated stage [FIG. 2.1(i), (j)]

Diameter 1260-1940 μm; *n* = 45 oocytes, 4 ovaries. The oocyte rapidly increases in size due to the uptake of fluid. Consequently, both the zona radiata (*c*. 30 μm thick) and follicular layer become thin and stretched, and the filaments spread out from each other. The cytoplasm takes on a homogeneous pale pink appearance.

2.3.2 OOCYTE FILAMENTS

Images from TEM demonstrated that, by staining with RR, the sectioned filaments have a glycocalyx of mucopolysaccharides coating their surface. This adhesive appears as a tangled mat of densely stained material on the external surface of the oocyte, is produced during hydration of the oocyte and can be up to *c*. 0.5 μm in thickness (FIG. 2.2). The glycocalyx was only visible in TEM-sections that were stained with RR since it tends to collapse and condense during the dehydration process in the absence of a suitable fixative and stain and it is too thin to be seen with conventional light microscopy even after staining with AB-PAS.

The filaments, which were tightly wound around the oocyte, begin to dissociate from the deteriorating follicular layer once the oocyte becomes fully hydrated, and then protrude freely from the oocyte surface (FIG. 2.3). The observation of a complete follicular layer surrounding the developing oocyte followed by its deterioration when the oocyte becomes hydrated corresponds to the histological description of postovulatory follicles in the hemiramphid, *Hemiramphus brasiliensis*, given by McBride & Thurman (2003). Therefore, this structure is presumed to be the postovulatory follicle.

2.3.3 PROPORTION AND SIZE DISTRIBUTION OF OOCYTES

Perinucleolar oocytes were numerically dominant in histological preparations of ovarian stages II-VIII (FIG. 2.4). The frequency of perinucleolar oocytes progressively decreased from 84% in stage II to 39% in stage VII ovaries as a result of maturation into more advanced oocytes, before rising sharply to 88% in stage VIII. In contrast, yolk vesicle oocytes remained relatively constant between 16 and 22% during stages II-VII before falling marginally to 10% in stage VIII. Yolk globule oocytes made up only a small proportion of the total oocytes (<5%) from when they first appeared in stage III. Relatively few oocytes were in the yolk globule stage, indicating that this stage of oocyte development is brief; their presence marks

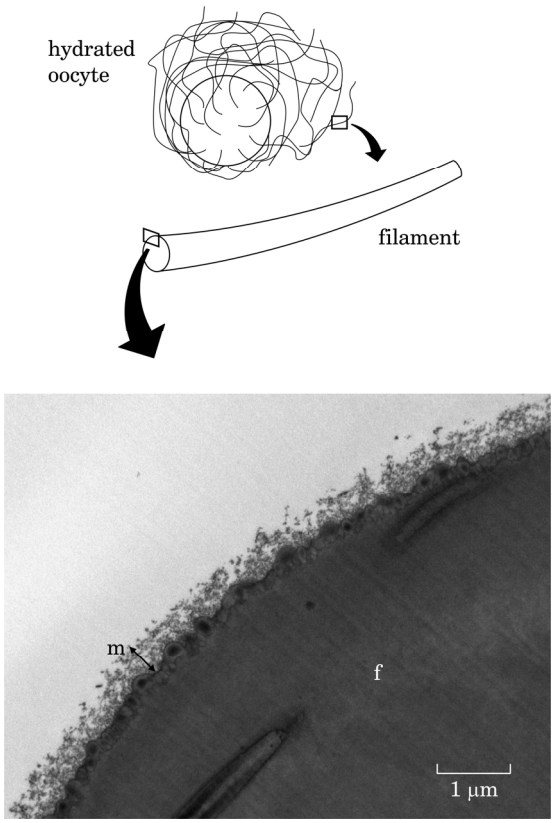

FIG. 2.2 Partial cross section of an oocyte filament (*f*) from a hydrated oocyte of *Hyporhamphus melanochir* stained with ruthenium red showing the adhesive layer of mucopolysaccharides (*m*). A line drawing of an ovulated oocyte and filament is included to orientate the image.

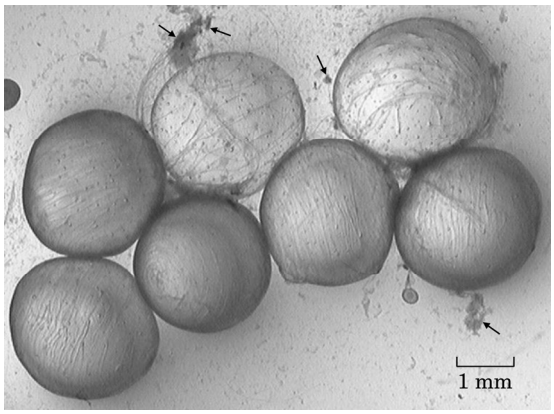

FIG. 2.3 Hydrated oocytes (two ovulated, five unovulated) teased out from a running ripe ovary of *Hyporhamphus melanochir*. Note: the remnant material from deterioration of the follicular layer, i.e. postovulatory follicle, indicated by arrows.

the beginning of vitellogenesis, which corresponds to reproductive maturity in stage III. Migratory nucleus oocytes were also present from stage III onwards. The frequency of these oocytes progressively increased from 6% in stage III to 18% in stage V until they underwent hydration during stages VI and VII. Yolk globule and migratory nucleus oocytes occurred at

low percentages in stage VIII ovaries; macroscopic examination of these ovaries sometimes revealed a few residual hydrated oocytes, which were otherwise absent.

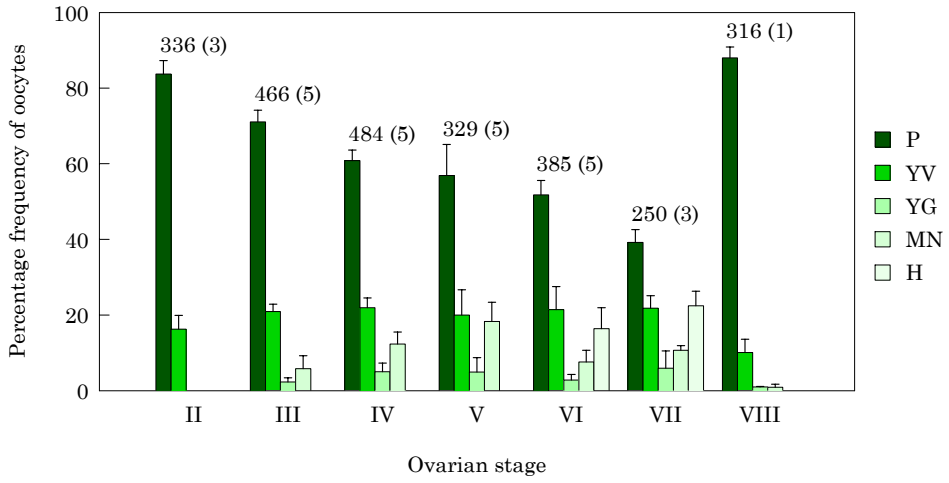

FIG. 2.4 Percentage frequencies of oocyte developmental stages (mean + 1 S.D.) in ovaries of *Hyporhamphus melanochir*. Abbreviations for oocyte stages: *P* perinucleolar; *YV* yolk vesicle; *YG* yolk globule; *MN* migratory nucleus; *H* hydrated. Numbers of oocytes and ovaries (in parentheses) are given for each ovarian stage.

The size distributions of oocytes in ovarian stages II-VII reveal a well-defined mode at <150 μm representing the perinucleolar oocytes, from which later-stage oocytes are recruited (FIG. 2.5). A bimodal distribution is evident in stage II ovaries, the second mode at *c*. 550 μm consisting of yolk vesicle oocytes. Yolk globule and migratory nucleus oocytes occur throughout the remaining ovarian stages. The mode that represents yolk globule oocytes is inconspicuous (*c*. 800 μm), presumably due to considerable size overlap with the preceding yolk vesicle oocytes and the brevity of the yolk globule stage, while the diameters of migratory nucleus oocytes are quite variable with a mode of *c*. 1500 μm. In stage VI and VII ovaries, a gap has emerged between the migratory nucleus oocytes and a group of oocytes with a mode of *c*. 2500 μm that have become rapidly hydrated.

The single largest oocyte for fresh and preserved samples from different fish was 3190 and 2762 μm, respectively. As a result of fixing in Gilson's solution, only hydrated oocytes with diameters >2200 μm underwent significant shrinkage (by a factor of 0.87) [ANOVA, $F_{1,78} = 59.6$, $P<0.001$], while earlier-stage oocytes generally remained the same size.

The more advanced oocytes of each ovarian stage were present in relatively low frequencies and consequently appear insignificant by numerical comparison alone. However, the significance of the advanced group is emphasized by calculation of the proportional volumes of oocyte size classes (FIG. 2.5), particularly when it is considered that one ripe oocyte of 3 mm diameter occupies the same volume as 2.7×10^4 perinucleolar oocytes of 0.1 mm diameter (i.e. 14.1 mm^3).

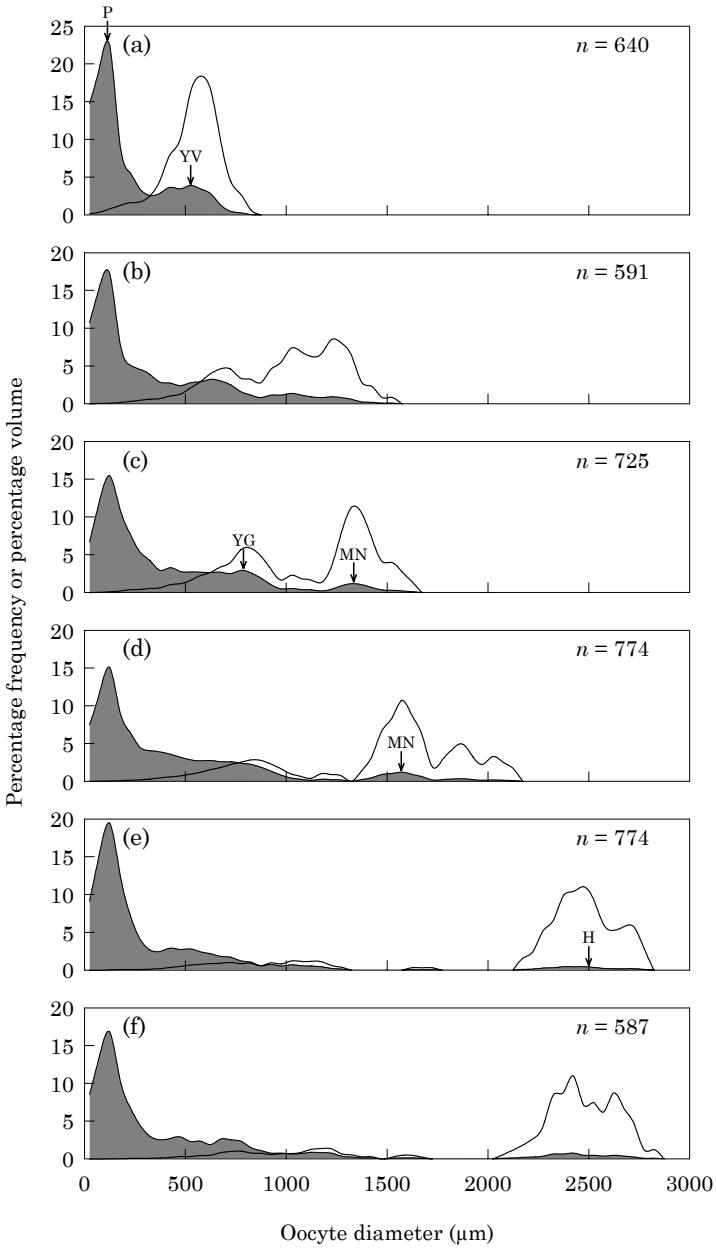

FIG. 2.5 Percentage frequency distributions of oocyte diameters (shaded area) and proportional volume (unshaded area) in ovaries of *Hyporhamphus melanochir*. Ovarian stages: (a) II; (b) III; (c) IV; (d) V; (e) VI; (f) VII. Abbreviations for oocyte stages as for FIG. 2.4. Number of oocytes is given for each ovarian stage. Data are presented for 50-μm size classes and smoothed with a moving average of three.

2.3.4 SEXUAL MATURITY AND FECUNDITY

For calculation of size at sexual maturity, female *H. melanochir* were considered mature if their ovaries were macroscopically classified as stage III or above. The L_{50} was estimated to be 192.7 mm L_S by the logistic function fitted to binary response data, $P_M = 1/[1+e^{-(-17.150+0.089L_S)}]$ (FIG. 2.6).

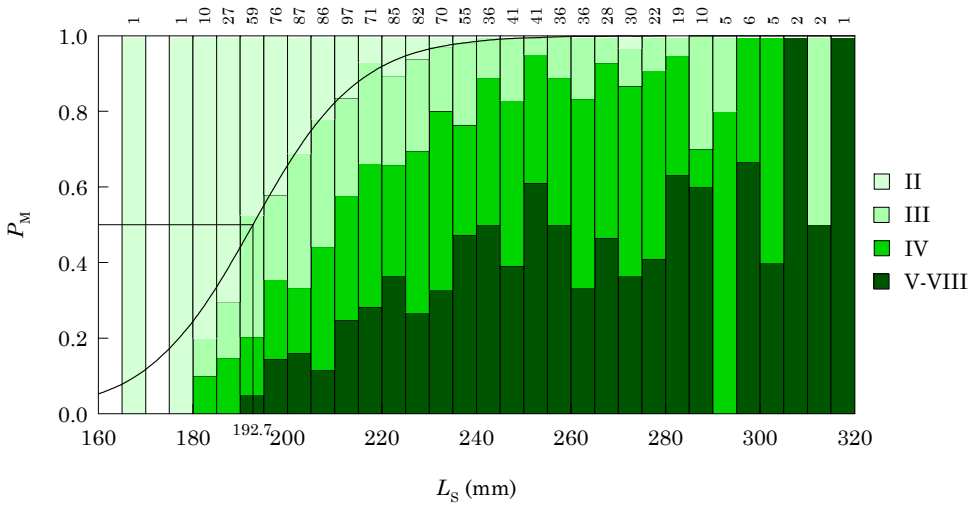

FIG. 2.6 Proportions of ovarian stages by standard length (L_S) class of *Hyporhamphus melanochir*. Also shown is the logistic curve that estimates the probability that females are mature at a given L_S. The vertical drop line indicates L_{50}. Number of fish is given for each L_S class.

Individual estimates of F_B (n = 56) ranged from 201 (206 mm L_S, 67.2 g W_T) to 3044 oocytes (264 mm L_S, 135.9 g W_T). Hydrated oocytes (>2200 µm) were generally from stage VI or VII ovaries; otherwise a few were from stage V. The relationships between F_B and length and weight of these fish (197-287 mm L_S; 43.7-155.7 g W_F) are described by the equations: $\log_{10}F_B = 4.989 \log_{10}L_S - 8.895$ ($r^2 = 0.734$, $P<0.001$) and $\log_{10}F_B = 6.879 \times 10^{-3} W_F + 2.330$ ($r^2 = 0.631$, $P<0.001$) (FIG. 2.7). Relative batch fecundity (i.e., F_B/W_F) was significantly correlated but a poor predictor of W_F ($r^2 = 0.146$, $P<0.01$, data not shown), and ranged from 3.2-27.2 oocytes g^{-1}, with a mean (± 1 S.E.) of 11.5 ± 0.6 oocytes g^{-1}.

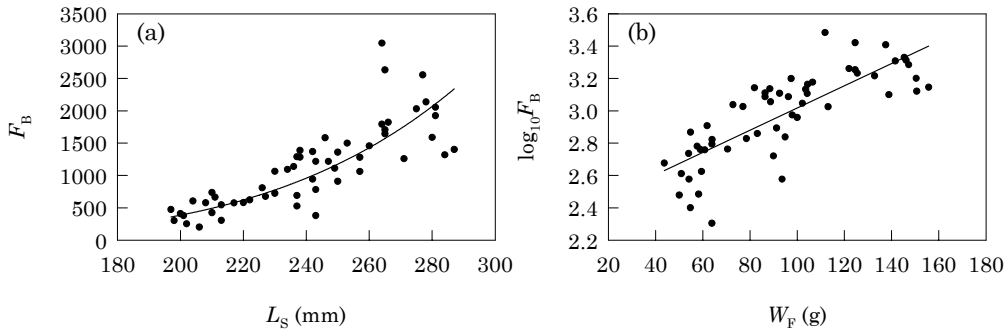

FIG. 2.7 Relationships between (a) batch fecundity (F_B) and standard length (L_S) and (b) $\log_{10}F_B$ and ovary-free fish weight (W_F) of *Hyporhamphus melanochir*. See text for regression and correlation results.

2.3.5 FEMALE-MALE CHARACTERISTICS

Females generally dominated the collection (72.6% females *v*. 26.5% males, 0.9% immature or unknown sex, n = 2000). The female-to-male sex ratio was significantly higher

(4.5:1) for the spawning season compared to the non-spawning season (1.2:1) (TABLE 2.3). A 250 mm L_S individual collected in March was classified as bisexual since the gonads consisted of both female and male reproductive tissue.

TABLE 2.3 Monthly sex ratios of *Hyporhamphus melanochir* and results of chi-square (χ^2) goodness of fit tests.

Month	Females	Males	♀:♂	χ^2
Spawning season				
October	147	29	5.1:1	79.1***
November	146	13	11.2:1	111.3***
December	242	33	7.3:1	158.8***
January	184	60	3.1:1	63.0***
February	204	41	5.0:1	108.4***
March	205	76	2.7:1	59.2***
Non-spawning season				
April	122	102	1.2:1	1.8
May	52	27	1.9:1	7.9**
June	28	21	1.3:1	1.0
July	22	29	0.8:1	1.0
August	50	48	1.0:1	0.0
September	50	50	1.0:1	0.0

**P<0.01, ***P<0.001.

2.3.6 REPRODUCTIVE SEASONALITY

Despite large fluctuations with successive weekly samples, mean I_G values for both females and males indicated a spawning season from October to March (FIG. 2.8). This spawning season was clearly separable from the non-spawning season by I_G values averaging >2.5% for females and >0.5% for males. It appears there are interannular differences in I_G for females, however, a moving average throughout the sampling period reveals that overall the consecutive spawning seasons are actually similar, and that the extent of the fluctuations within a season can be attributed to the gonad stage proportions varying greatly and inconsistently between samples. On an individual basis, I_G reached a maximum of 21.6% for females and 3.4% for males, while the largest pairs of ovaries and testes weighed 27.7 and 3.5 g, respectively.

A protracted spawning period was also evident in the monthly percentage frequencies of ovarian stages. Most females sampled during the non-spawning season (90%) were developing virgins, mature virgins or recovering (stages II and III), while most during the spawning season (62%) were mature, ripe or running ripe (stages IV-VII) (FIG. 2.9). All of stages II-VII occurred throughout the spawning season, except in January, when no fish were running ripe (stage VII). In September approaching the next spawning season, a small number of females had ripe ovaries (stage VI), although none were running ripe. Spent ovaries (stage VIII) mainly appeared late in the spawning season during February and March and persisted until April.

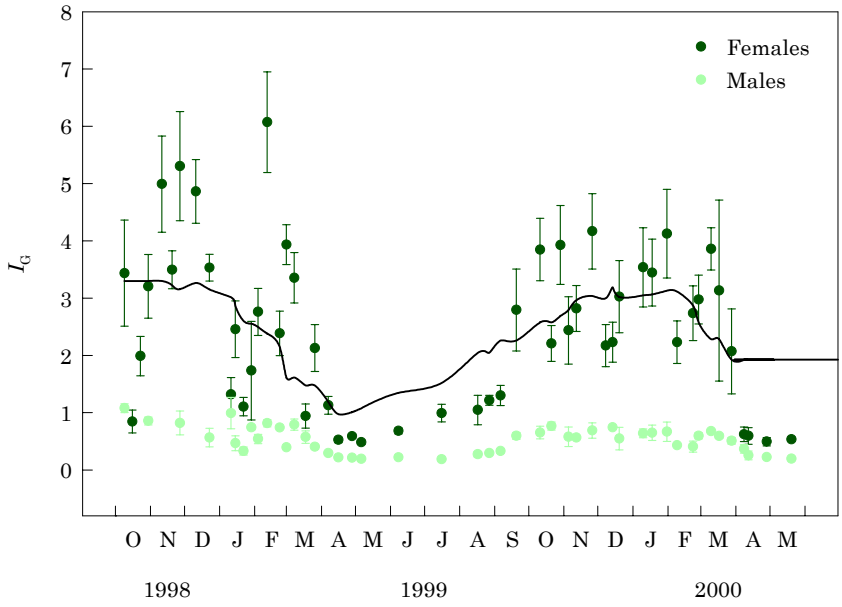

FIG. 2.8 Gonadosomatic indices (I_G, mean ± 1 S.E.) for female and male *Hyporhamphus melanochir* from October 1998 to May 2000. To improve clarity of presentation, data for the December 2001 sample was excluded. The spline curve represents the moving average of female I_G with a sampling proportion of 0.2.

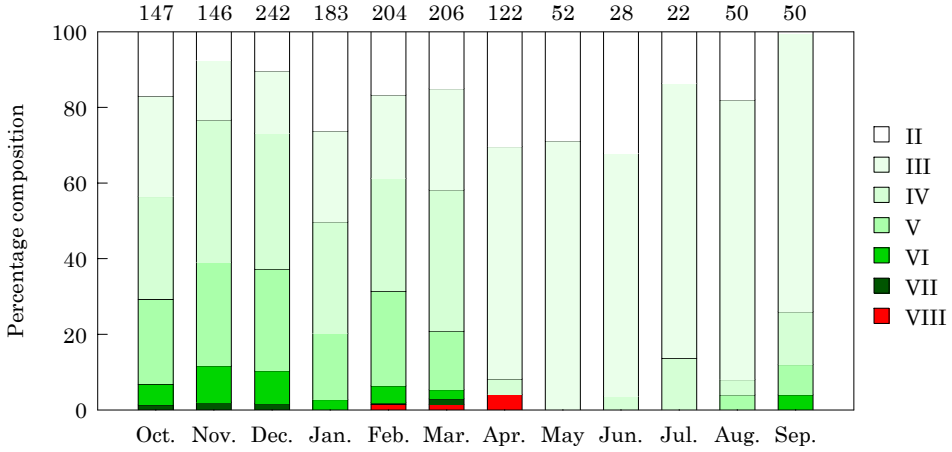

FIG. 2.9 Monthly percentage compositions of ovarian stages of *Hyporhamphus melanochir*. Data were pooled for a calendar year. Number of fish is given for each month.

Average maximum diameters of fresh oocytes ranged from 214-2937 µm for individual fish with stage III and VII ovaries, respectively. The monthly trend for diameters of the most advanced oocytes was similar to that of I_G values, with spawning and non-spawning seasons clearly defined (FIG. 2.10). Oocyte diameters were highest during the spawning season, ranging from 1208-1355 µm in December and March, respectively, before declining sharply to *c.* 450 µm in April and May. From May onwards, the diameter progressively increased until the start of the next spawning season in October.

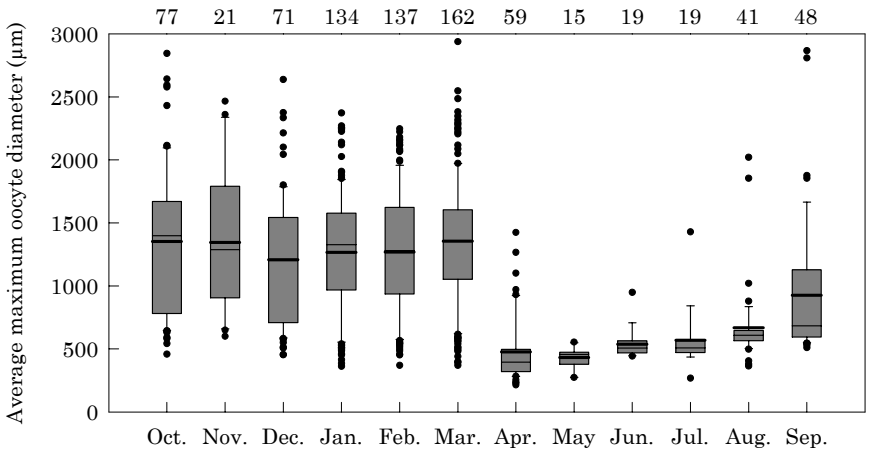

FIG. 2.10 Monthly distributions of average maximum oocyte diameters of *Hyporhamphus melanochir*. Boxes enclose values between the 25th and 75th percentiles; whiskers are the 10th and 90th percentiles; thin and thick horizontal lines are median and mean values, respectively; and each data point is an outlier representing one fish. Data were pooled for a calendar year. Number of fish is given for each month.

2.4 DISCUSSION

This study provides the first histological description of oocytes of *H. melanochir* and demonstrates that the developmental events observed in these oocytes are very similar to those described for most other oviparous teleosts (Wallace & Selman, 1981; deVlaming, 1983; Tyler & Sumpter, 1996). Based on the classification scheme and terminology used by West (1990), five stages of oocyte development were identified: perinucleolar, yolk vesicle, yolk globule (vitellogenic), migratory nucleus and hydrated stages. Perinucleolar oocytes and yolk vesicle oocytes were found in all ovaries of stage II onwards. The formation of yolk globules marks the beginning of vitellogenesis (and ovaries are considered mature, i.e. stage III). Once yolk accumulation is completed, coalescence of yolk and migration of the nucleus occur simultaneously. The maturation process ends when the oocyte hydrates and is ovulated. Descriptions of these five histological oocyte stages closely correspond to the four groups of whole oocytes classified in a ripe ovary by Ling (1958; TABLE 2.4): perinucleolar oocytes are referred to as 'immature;' yolk vesicle and yolk globule oocytes are 'maturing;' migratory nucleus oocytes are 'mature;' and hydrated oocytes are 'ripe.' The single grouping of yolk vesicle and yolk globule oocytes is probably due to considerable size overlap. The demonstrated coherence between histological and whole oocyte descriptions has important implications for reproductive studies of *H. melanochir* where histology is not available since the macroscopic staging of ovaries is dependent upon accurate classification of the most advanced oocytes present.

TABLE 2.4 Classification and description of whole oocytes within ripe ovaries of *Hyporhamphus melanochir* (reproduced with permission from Ling, 1958).

Classification	Whole oocyte description
Immature	Very small, angular. Transparent, nucleus clearly visible. Diameter up to 0.2 mm.
Maturing	Small, opaque, diameter 0.2-1.0 mm. The smallest of this group are beginning to accumulate yolk globules, while larger oocytes are quite opaque (nucleus not visible).
Mature	Large, opaque, pale yellowish in colour, diameter up to 1.6 mm. Smaller oocytes sometimes overlap with maturing oocytes.
Ripe	Very large, transparent, diameter 2.5-3.5 mm. Covered by adhesive filaments equal in length to oocyte diameter. Oocytes lie free within lumen and are easily stripped from a ripe female.

The pattern of development of oocytes within the ovary of *H. melanochir* has been described as asynchronous (Ling, 1958; St Hill, 1996). However, since at least two distinct groups or clutches of oocytes are distinguished at any time in mature ovaries of *H. melanochir*, this pattern should be interpreted as group-synchronous oocyte development (Wallace & Selman, 1981). Group-synchronous oocyte development has been reported in other hemiramphids (*He. brasiliensis* and *He. balao*, McBride & Thurman, 2003). Although the size distributions of oocytes through ovarian development appear to be almost continuous, except for the temporary gap that emerges between hydrated and migratory nucleus oocytes prior to spawning, the distinctness of the cohorts of oocytes is somewhat masked due to the measurement of oocytes from several ovaries that were likely to be at slightly different stages of developmental despite being classified as the same macroscopic ovarian stage. This has the effect of flattening out the distributions of the individual cohorts compared to when oocytes are measured from only one ovary. The co-occurrence of all oocyte stages in the ripe ovary and the presence of advanced yolk-stage oocytes in spent ovaries indicate indeterminate fecundity and a capacity for multiple spawning within the reproductive season (Hunter & Macewicz, 1985).

Based on the presence of hydrated oocytes, and assuming this batch of oocytes will be released in the next spawning event, batch fecundity for individual fish ranged from 201-3044 oocytes, depending on fish size (length more so than weight). However, relative batch fecundity was independent of fish weight, indicating that *H. melanochir* of different sizes invested proportionally similar energy levels for maturation of oocytes. Fecundity estimates for *H. melanochir* from earlier studies ranged from 1280-3000 (Thomson, 1957*b*) and 9000-10000 oocytes (Ling, 1958). However, these results are questionable since Thomson (1957*b*) counted non-hydrated oocytes that were only 1.5 mm in diameter, which correspond to migratory nucleus oocytes in the present study, while Ling (1958) sampled relatively few fish and did not specify whether hydrated oocytes or total oocytes were counted.

Assuming *H. melanochir* is a multiple spawner with indeterminate fecundity, the annual fecundity is a function of batch fecundity and spawning frequency (Hunter *et al.*, 1985;

Hunter & Macewicz, 1985); however, spawning frequency is yet to be determined. Estimates of spawning frequency require either validation of the duration of the hydrated stage (hydrated oocyte method), or the identification and classification of the postovulatory follicle deterioration and resorption processes into a series of distinct histological stages, each with an assigned age since spawning (postovulatory follicle method) (Hunter & Macewicz, 1985). The observed remnant material following deterioration of the follicular layer around the hydrated oocyte was identified as the postovulatory follicle, which indicates that spawning had occurred or was imminent (Saidapur, 1982; Hunter & Macewicz, 1985). Although postovulatory follicles of *H. melanochir* were easily identified using light microscopy, none were found in any prepared ovarian sections, and so characterisation based on histology was not possible.

According to data from this study, the new legal minimum length of 230 mm L_T (= 198 mm L_S) would allow 62.1% of females to reach maturity before they can be legally taken [*cf.* only 25.8% at the old legal length of 210 mm L_T (181 mm L_S)]. However, the haul net mesh size regulation of 30-32 mm remains unchanged, and it is not yet known the survival of released undersized fish after being handled, or the effect the change in legal length has on the population. Preliminary observations in the laboratory suggest that *H. melanochir* suffer high mortality rates from scale loss after handling (personal observation). The L_{50} of 193 mm in this study was 56.4% of the length of the largest female examined (342 mm L_S). The corresponding age at maturity (i.e. t_{50}), based on an age-length key for female *H. melanochir* from Gulf St Vincent (Ye *et al.*, 2002*b*), is estimated to be 20.5 months. To my knowledge, no study of hemiramphids, except McBride & Thurman (2003), has determined size at maturity with the precision reported here, but other studies have reported the size of the smallest females with hydrated oocytes. The smallest running ripe female in Ling's (1958) study was 216 mm caudal fork length (equivalent to 199 mm L_S, unpubl. data), which is comparable to our estimate of L_{50}. Regardless of the method used, the size at maturity is close to 60% maximum body size for a number of hemiramphids [56.8% for *H. melanochir* (Ling, 1958); 58.2% for *He. limbatus* (Silva & Davies, 1988); 58.0% for *Zenarchopterus kampeni* (Coates & Van Zwieten, 1992); 63.3% for *He. brasiliensis* and 58.6% for *He. balao* (McBride & Thurman, 2003)], and McBride & Thurman (2003) noted the potential usefulness of this percentage value for predicting size at maturity of any hemiramphid that has not been studied.

Sex ratios of *H. melanochir* ≥210 mm L_T were biased strongly toward females during the spawning season, which were found, from other independent surveys, to form large schools in relatively shallow waters (Ye *et al.*, 2002*a*). It is unlikely that the skewed sex ratios were an artefact of the sampling gear (Rollefsen, 1953) because the haul nets used were presumed to have effectively fished the entire environment to its depth of <5 m. This, along with sex ratios approximating 1:1 during the non-spawning season, suggests that for *H. melanochir* there is a

spatial segregation of sexes into spawning shoals. The predominance of males or females in spawning shoals has been documented for *H. melanochir* (Ling, 1958) and several other hemiramphids (Talwar, 1962*b*; Talwar, 1967; Durai *et al.*, 1988; Morgan & Trippel, 1996). However, a more detailed ecological study on the spatial and temporal patterns of distribution of sexes, or perhaps spawning behaviour itself, is necessary to explain this phenomenon. The occurrence of only one bisexual fish in the samples indicates that hermaphroditism is rare, and so *H. melanochir* are characterised as gonochoristic (Sadovy & Shapiro, 1987).

The spawning season described in this study agrees with the South Australian population of *Reporhamphus melanochir* (= *H. melanochir*) studied by Ling (1958). Increases in I_G values and average maximum diameter of oocytes, and the presence of ripe, running ripe or spent ovaries indicate that the spawning season of *H. melanochir* is protracted, extending for at least six months from October to March, with ovarian maturation in a few fish in late September and early April. A slightly shorter spawning duration (October to February) was reported by Thomson (1957*b*) and Jordan *et al.* (1998) for *H. melanochir* populations from W.A. and Tas., respectively. However, results from these studies are inconclusive since they were based on the presence of 'ripe' oocytes 1.5 mm in diameter (Thomson, 1957*b*) and an incomplete dataset for March (Jordan *et al.*, 1998). A protracted spawning season is further supported by the occurrence of *H. melanochir* larvae among plankton samples collected throughout Gulf St Vincent during this extended period (Noell, 2003; Chapter 5). Ye *et al.*, (2002*a*) noted two 'distinct' peaks within the spawning season for *H. melanochir*, however, this conclusion was interpreted from sampling that was undertaken on a monthly basis. Close inspection of weekly data in this study show that these peaks are not real, but instead a result of considerable variation and fluctuation in gonadosomatic indices within each month. The failure to detect any underlying reproductive cycle of shorter periodicity by sampling on a weekly basis (e.g. lunar or other environmental cycle), along with the co-occurrence of all mature ovarian stages in many samples during the spawning season, suggests a lack of population synchrony in gonad development.

Determining the combination of environmental factors that influence the time and duration of spawning is beyond the scope of this study. However, since the spawning months coincide with increased day length (Geoscience Australia, 2002) and water temperature (AODC, 2002) in the gulf region relative to the quiescent period, gonadal recrudescence in *H. melanochir* may be stimulated by increases in these variables. Such increases appear to be the predominant environmental cues responsible for stimulating gonadal recrudescence in many teleosts in temperate waters (Lam, 1983; Bye, 1984). The timing of spawning in *H. melanochir* may also be linked to the timing of the summer/autumn bloom in productivity of zooplankton in the coastal shelf waters of central and western S.A. (Ward & McLeay, 1999; Ward *et al.*, 2001) since zooplankton appears to be an essential food source for *H. melanochir*

larvae (see Chapter 6). As the duration of the peak productivity can be variable over successive years, multiple spawnings during a protracted spawning season may be a critical 'bet-hedging strategy,' particularly for low fecund species with large eggs, such as *H. melanochir*, as it would ensure suitable feeding conditions for as many larvae as possible and guard against mass mortality/predation in a fluctuating environment (Lambert & Ware, 1984).

The Hemiramphidae are of particular interest when studying trade-offs in reproductive traits due to large variations in egg size, fecundity, and reproductive mode of its species. For example, the diameters of hemiramphid eggs range from 1.1 to 3.5 mm, the attaching filaments range in length from 0.05 to 60 mm and vary in arrangement, and reproductive modes include the production of demersal eggs, buoyant pelagic eggs, or precocious young (Collette et al., 1984; McBride & Thurman, 2003). In the case of *H. melanochir*, most of the early life-history traits possessed suggests that, along the continuum of the traditional paradigm of *r*- and *K*-selection (proposed by MacArthur & Wilson, 1967), this species is characterised as a *K*-strategist. Its eggs are large (*c.* 3 mm in diameter, Jordan et al., 1998) and a more advanced stage of development is reached in larvae at hatching (Jordan *et al.*, 1998; Noell, 2003).

The large eggs of *H. melanochir* are a noteworthy feature. The production of relatively few large demersal eggs suggests that *H. melanochir* conform to the inverse relationship between number and size of eggs that generally occurs in teleost fish, probably as a result of morphological constraints of body size (Duarte & Alcaraz, 1989; Elgar, 1990). The greater amount of yolk in large eggs provides more energy for growth and development before the larvae requires exogenous nutrition, resulting in larger, well-developed larvae at hatching and at first feeding. This offers several vital benefits: larvae emerge with a better repertoire of behavioural and physiological capabilities than less developed larvae from smaller eggs; they are more resistant to starvation because weight-specific metabolic rates are lower and bodily energy stores are greater; and the larval period is shorter (Blaxter, 1988; Fuiman, 2002).

Consequent to the inverse relationship between fecundity and egg size, it has been suggested (Pepin & Myers 1991, Mertz & Myers, 1996), and demonstrated empirically (Ricker *et al.*, 2000), that species with low fecundity show less interannual variability in egg production (and *vice versa*). As such, this positive correlation could influence variations in year-class strength and ultimately recruitment into the adult population. However, in addition to fecundity, fluctuations in recruitment are probably determined by the interplay of other life history traits and environmental variability. For example, recruitment variability in marine fishes has also been examined in the contexts of egg and larval size (Rothschild & DiNardo, 1987; Miller *et al.*, 1988; Pepin & Myers, 1991), mortality rates during the early life stages (Houde, 1987; Bradford, 1992; Bradford & Cabana, 1997), the timing of spawning relative to seasonal productivity of food items (Cushing, 1969, 1990; Pepin, 1990; Mertz & Myers,

1994), the effect of environmental factors on survival of various early life stages (Lasker 1978; Bradford & Cabana 1997; Myers, 1998), and through the development of stochastic recruitment models (Fogarty *et al.*, 1991). Therefore, a much greater understanding of the biology and ecology of *H. melanochir* is required before the complex issue of recruitment variability can be resolved for this species.

The oocyte filaments of *H. melanochir* are very similar in morphology to those described for other fish species with such ornamentation (e.g. *Belone belone*, Donato *et al.*, 1978; *Odonthestes bonariensis*, Guandalini *et al.*, 1994). Observations of eggs of *H. melanochir* (Jordan *et al.*, 1998; pers. observ.) and other marine hemiramphids (e.g. Berkeley & Houde, 1978) attached to seagrass and algae suggest that the function of these filaments is attachment to vegetation. Many other examples exist in the literature of filaments on the eggs of different fish species, all of which serve a similar function in allowing the egg to attach to substrate, thereby increasing its chances of survival, e.g. blenniids (Patzner, 1984), cichlids (Busson-Mabillot, 1977, as cited in Riehl & Appelbaum, 1991), gobiids (Takahashi, 1978; Riehl, 1984), cyprinodontids and oryziids (Dumont & Brummet, 1980; Hart *et al.*, 1984) and pseudochromids (Mooi, 1990). The additional finding that the oocyte filaments of *H. melanochir* have an outside layer of polysaccharides indicates that the mode of attachment is by adhesion as well as entanglement, an adaptation which would supposedly increase the probability that the demersal eggs will become attached to vegetation before they reach the bottom. This trait not only prevents the eggs from being covered by sediment, it also minimises the risk of predation, especially where parental care is reduced or absent (Potts, 1984).

Most beloniform fishes are oviparous, spawning large demersal eggs with attaching filaments, characters they share with other atherinomorph fishes (Rosen & Parenti, 1981). The eggs typically require relatively long incubation periods of one to two weeks (Kovalevskaya, 1982), and the larvae are well formed and capable of actively capturing food at hatching. Although not a teleost, the southern calamary (*Sepioteuthis australis*) is another key species within the South Australian Marine Scalefish Fishery that appears to be somewhat dependent on vegetation for spawning, and thus it is interesting to compare its early life history with that of *H. melanochir*. It has been suggested that the habitat in which eggs are spawned explains the diversity of eggs, larvae, and reproductive styles in fishes (Kryzhanovskii, 1949). Accordingly, a comparison between the life histories *H. melanochir* and *S. australis* reveal a number of similarities in their traits, i.e. the production of relatively few large eggs, the attachment of eggs to seagrass (e.g. *Zostera* spp.) or algae (Jones *et al.*, 1990; Parry *et al.*, 1990), a protracted spawning period (Jones *et al.*, 1990), a long incubation period (Winstanley *et al.*, 1983), well-developed larvae that swim to the surface soon after hatching, fast-growth, and a short life span. Therefore, by demonstrating similar traits, it appears that these two

species conform to this theory by adopting the same strategy to optimize early survivorship, i.e. approaching a *K*-strategy (discussed earlier), which is typical among species that thrive in the presence of suitable habitat and stable environmental conditions (Fuiman, 2002).